JASR 7969
1 September 2005; Disk Used
ARTICLE IN PRESS
No. of Pages 8, Model 5+

ELSEVIER

Available online at www.sciencedirect.com
SCIENCE DIRECT®

Advances in Space Research xxx (2005) xxx–xxx

ADVANCES IN SPACE RESEARCH
(a COSPAR publication)
www.elsevier.com/locate/asr

On the occurrence of auroral westward flow channels and substorm phase

M.L. Parkinson [a,*], P.L. Dyson [a], M. Pinnock [b]

[a] Department of Physics, La Trobe University, Melbourne, Victoria 3086, Australia
[b] British Antarctic Survey, Natural Environment Research Council, Cambridge CB3 0ET, UK

Received 8 July 2004; received in revised form 12 May 2005; accepted 16 August 2005

Abstract

Auroral westward flow channels (AWFCs) are intense, narrow channels of westward drift overlapping the equatorward edge of the auroral oval in the pre-magnetic midnight sector. They are a close relative of the sub-auroral polarisation stream which encompasses polarisation jets, a phenomenon also known as sub-auroral ion drift events. Recent observations made with the Tasman Geospace Environment Radar (TIGER) (147.2°E, 43.4°S Geodetic; 55.0° Geomagnetic) have revealed close associations between the appearance of AWFCs and substorm onset, and their subsequent decay toward the end of recovery phase. In fact, in terms of electric field strength, they are the strongest signatures of substorms in the ionospheric convection (>50 mV m). In terms of electric potential difference (>10 kV), they also represent a substantial fraction of the total potential difference generated during substorms. The AWFCs exhibit a diverse range of behaviour, there being no typical event. The radar observations show that radial polarisation fields sometimes oscillate towards and away from the Earth, and bifurcate, within regions of closed flux in the magnetotail throughout substorm evolution. We have identified every AWFC observed by TIGER during the first year of operation, 2000. Simple statistical arguments imply that one, if not more, AWFC probably occurs during every substorm. AWFCs are a fundamental aspect of substorm evolution.

Keywords: Auroral ionosphere; Electric fields and currents; Ionosphere–magnetosphere interactions; Storms and substorms

1. Introduction

Polarisation Jets (PJs) were discovered by Galperin et al. (1973). They are narrow channels (<1–2°Λ) of intense westward plasma flow (500 m s to >4 km s) which occur just equatorward of, or overlapping, the equatorward edge of the auroral oval in the evening sector (Karlsson et al., 1998). PJs are also known as sub-auroral ion drift events (SAIDs) (Spiro et al., 1979; Anderson et al., 1991, 1993, 2001). Substorm-associated radar auroral surges (SARAS) (Freeman et al., 1992; Shand et al., 1998) probably represent a different aspect of PJ/SAIDs. The term "sub-auroral polarisation stream" (SAPS) (Foster and Burke, 2002) has been proposed to encompass these phenomena, as well as the weaker background westward flows (∼100–400 m s) which persist beyond midnight, and immediately equatorward of the eastward circulation within the dawn convection cell.

The Tasman International Geospace Environment Radar (TIGER) (147.2°E, 43.4°S Geodetic; 55° Geomagnetic) (Dyson and Devlin, 2000) is a recent addition to the Super Dual Auroral Radar Network (SuperDARN). A description of SuperDARN radar design and operation has been given by Greenwald et al. (1985, 1995). Auroral westward flow channels (AWFCs) were recently discovered using TIGER (Parkinson et al., 2003). AWFCs are probably also a different aspect of PJ/SAIDs. However, AWFCs appear between the onset and recovery of magnetospheric substorms, whereas satellite observations have shown that PJ/SAIDs appear during the recovery phase (Anderson et al., 1993). When SuperDARN radars are deployed equatorward of TIGER, it will be interesting to see whether they also observe peak PJ/SAID velocities during the recovery phase.

* Corresponding author.
E-mail address: m.parkinson@latrobe.edu.au (M.L. Parkinson).

0273-1177/$30 © 2005 Published by Elsevier Ltd on behalf of COSPAR.
doi:10.1016/j.asr.2005.08.028

AWFCs are distinguished from reconnection-driven flow bursts in the return sunward (westward) circulation within the afternoon convection cell by their greater temporal persistence. AWFCs can extend over many hours of longitude in the afternoon to post-midnight sector, and can last for several hours. However, short-lived westward flow bursts were seen to expand equatorward through the return sunward flow, feeding an AWFC (Parkinson et al., in press). The same event was observed simultaneously using the King Salmon radar. Analysis of this event showed that magnetic conjugacy was satisfied on large spatial and temporal scales (Parkinson et al., in press), consistent with the earlier results of Weimer et al. (1985).

Comparisons with DMSP particle precipitation data and IMAGE spacecraft global-scale FUV images show that AWFCs tend to overlap the equatorial edge of the auroral oval (Parkinson et al., 2003, in press). Like PJ/SAIDs (Karlsson et al., 1998), AWFCs have peak occurrence in the evening sector near 22 h magnetic local time (MLT). AWFCs are observed at the poleward limit of the occurrence distribution for PJ/SAIDs (Karlsson et al., 1998), and tend to overlap the equatorward edge of the auroral oval. AWFCs map to the inner magnetosphere in the sense of the inner edge of the central plasma sheet and Earthward towards the plasmapause.

Jayachandran et al. (2003) used ultraviolet imager data recorded on board the POLAR spacecraft to identify the onset signatures of many substorms. His E-region ionospheric signatures overlapped the equatorward boundary of the ion auroral oval in the evening sector, close to where AWFCs occur (an F-region phenomenon). For the two substorms shown by Jayachandran et al., the ionospheric signatures preceded the onset signatures at geosynchronous orbit by several minutes.

Substorm phase can be defined by negative bays in the geomagnetic X component measured by ground-based magnetometers at auroral latitudes. The onset times can be related to particle injections and dipolarisation events observed at geosynchronous orbit. Using these criteria, AWFCs are observed to start near to substorm onset and finish near to the end of recovery phase. In terms of electric field enhancements, AWFCs are the strongest manifestation of substorms in the inner magnetosphere (Parkinson et al., in press). The observations made so far naturally raise some important questions. Is every substorm accompanied by an AWFC? Do AWFCs and substorms occur independently of each other? Are AWFCs the cause or consequence of substorms, or both? That is, are AWFCs a fundamental aspect of the substorm process?

The purpose of this paper is to present simple statistical results which imply the occurrence of AWFCs is fundamental to substorm evolution. We will argue that one or more AWFC probably occurs for nearly every substorm. The numerous AWFCs identified also imply unexpected and diverse morphology of electric fields within the inner magnetosphere (as defined above).

2. Analysis and results

Fig. 1 shows a full-scan plot of the line-of-sight (LOS) Doppler velocity recorded during an AWFC event on 22 April 2000. Two main bands of ionospheric scatter were detected, one via 0.5-hop propagation at nearer ranges and another via 1.5-hop propagation at further ranges. The LOS velocities recorded in the latter band reveal anti-sunward drift in the polar cap on the western-most beams, becoming eastward flows at lower latitude on the eastern-most beams. On the other hand, the scatter at nearer ranges reveals strong westward drift bifurcated into two flow channels separated by 1–2° of latitude. AWFCs like this are observed frequently by the TIGER radar. Although full-scan plots of the backscatter parameters can be very informative, it would be extremely tedious examining many thousands of them to identify all of the AWFCs present in a database.

Hence, we developed methods to quickly identify all the AWFCs in the TIGER data base. This involved examining every range-time plot of LOS velocity recorded on beam 15 during the first year of radar operation, 2000. Beam 15 becomes a magnetic eastward beam at furthest ranges, and thus produces the clearest signatures of AWFCs (see Fig. 1 of Parkinson et al., 2003). The range-time plots were limited to the time interval 08–14 UT (~19–01 MLT), corresponding to the MLT sector where TIGER is most likely to observe AWFCs. The colour scale was adjusted so that echoes with approaching, westward velocities larger than 450 m s were coloured bright red, whereas weak receding velocities were coloured blue. AWFCs were then quickly recognised from bright red patches of ionospheric scatter at auroral and sub-auroral latitudes, often detached equatorward of blue scatter corresponding to eastward flow at higher latitude. The colour scale was chosen to emphasise flow reversal, a key feature helping to define the presence of AWFCs.

All 18.4 GB of FITACF data recorded during the year 2000 was analysed. Data-basing software was written to extract the time, group range, and LOS velocity of beam 15 results. This reduced the quantity of data to 35.2 MB, or approximately 3 MB per month. Thus daily range-time plots could be created. If there were doubts about whether an AWFC was present in the beam 15 plots, similar beam 0 plots were checked for inverted Doppler shifts consistent with a channel of enhanced westward drift. Conceivably, a computer program could be written to identify AWFC candidates on the basis of simple logical criteria, but we wanted to directly examine all events in this study.

Our first survey of year 2000 data revealed a significant number of clear AWFCs, but many less clearly defined events were recognised as our pattern recognition ability improved. It was realised that TIGER observed AWFCs at least every third night, much lower than the occurrence rate of substorms. There was also considerable diversity of morphology, with no “typical” event. A limited selection of

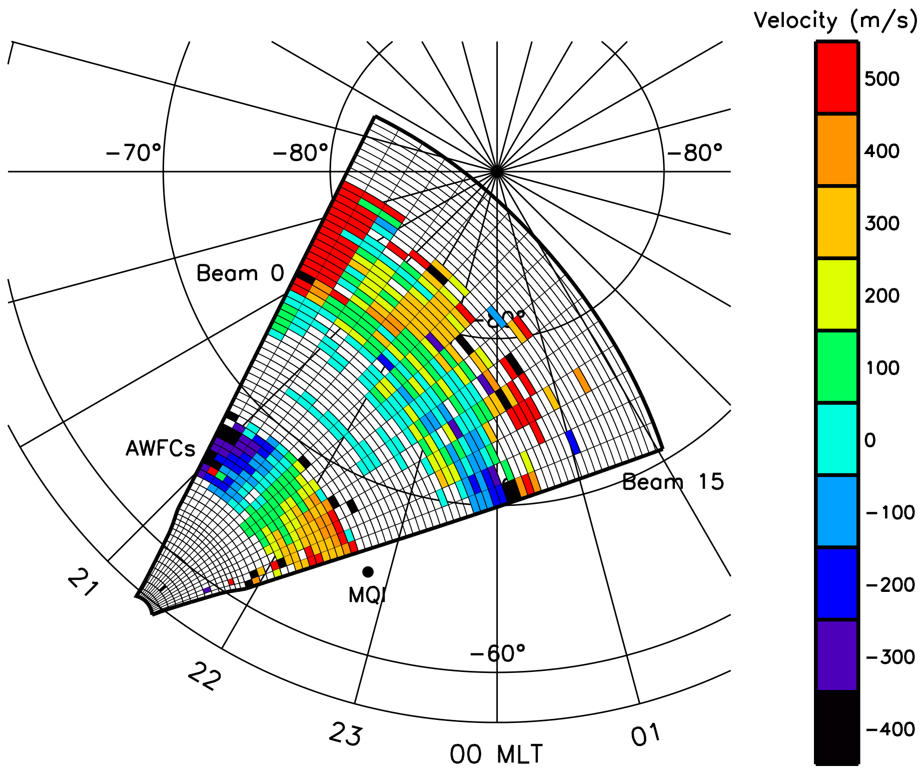

Fig. 1. Full-scan plot of the line-of-sight (LOS) Doppler velocity recorded by TIGER during 10:52–10:54 UT on 22 April 2000. Positive velocity (red) means that plasma was rapidly flowing toward the radar. The observations were mapped to a grid of magnetic local time and latitude. The location of Macquarie Island (MQI) magnetometer at the time of the radar observations is shown. (For interpretation of the references to colour in this figure legend, the reader is referred to the web version of this article.)

events illustrating the diverse range of morphology is shown in Fig. 2. As will be explained, the vertical lines indicate magnetometer signatures of substorm phase, as identified in Fig. 3.

The examples shown in Fig. 2 were not selected to illustrate that AWFCs are synchronised with substorms. The best such examples occur when isolated substorms occur and the radar is observing the pre-midnight ionosphere. However, the sequence of geomagnetic activity is often more complicated and leads to more interesting AWFC activity. Fig. 3 shows variations in the geomagnetic *X, Y*, and *Z* components measured by the fluxgate magnetometer on nearby Macquarie Island (54.5°S, 158.9°E; −65°Λ) for the same events and time intervals of Fig. 2. The onset (O), peak expansion (P), and end of recovery (R) substorm times have been inferred from the *X* -component deflections. However, Canadian magnetometer chain observations made further to the east were also consulted, as were energetic particle injections observed by the LANL satellites at geosynchronous orbit. For example, the onset at 08:00 UT on 6 April 2000 (Fig. 3(b)) was based upon an energetic particle injection identification.

The 3 April event (Fig. 2(a)) consisted of a succession of three relatively weak, equatorward expanding AWFCs. The largest velocities occurred just beyond peak expansion phase, but each episode was reasonably synchronised to the *X*-component deflections (Fig. 3(a)). The 6 April event (Fig. 2(b)) consisted of a thin "snake-like" AWFC expanding equatorward and contracting poleward. The two flow bursts commenced near to the two onset signatures, and the large velocities were established prior to the recovery phase (Fig. 3(b)). The large velocities were often confined to a channel of width less than a single range gate, or <45 km. The 22 April event (Fig. 2(c)) was broad and "jet like," consisting of at least two, latitudinally separated AWFCs imbedded within a decaying SAPS. The backscatter powers were also bifurcated, but are not shown for brevity. These scatter characteristics may indicate troughs within troughs (Galperin et al., 1986).

Clearly, the AWFC was established during the expansion phase and decayed toward the end of recovery phase. We identify the subsequent feature as a SAPS on the basis that it persists beyond the recovery phase, eastward of the Harang discontinuity and magnetic midnight, and equatorward of the flow reversal boundary. The latter is the separatrix between the predominant influence of reconnection-driven magnetospheric convection and the essentially co-rotational flows of the plasmasphere (cf. Parkinson et al., 2003, in press).

Finally, the 31 August event (Fig. 2(d)) revealed an initial thin, intense AWFC which expanded equatorward and

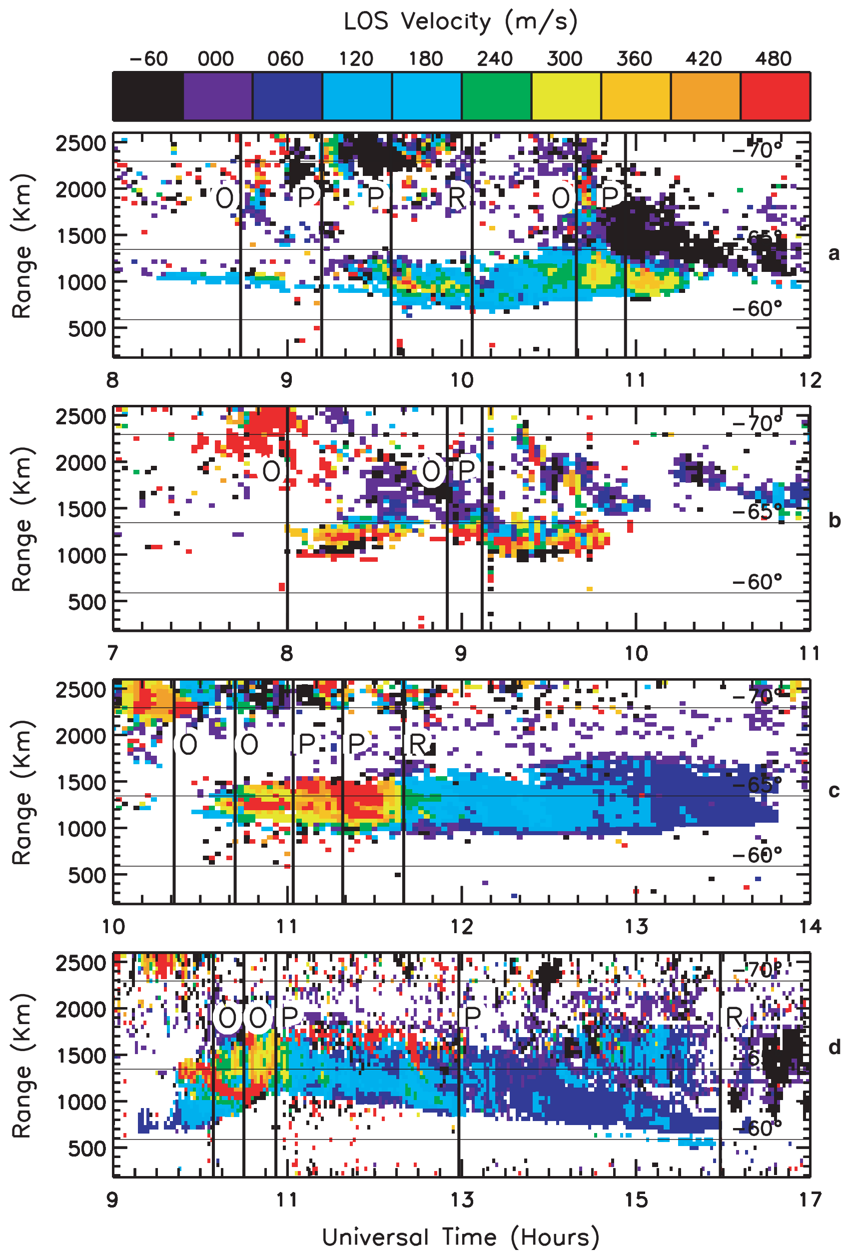

Fig. 2. A short compendium of AWFCs illustrating the diversity of morphology observed during the year 2000. Each panel shows the LOS Doppler velocity recorded on TIGER beam 15: (a) an episodic event observed during ~08:15–11:17 UT on 3 April; (b) a thin "snake-like" event observed during ~08:00–09:50 UT on 6 April; (c) a broad "jet-like" event observed during ~10:28–13:50 UT on 22 April; (d) an event exhibiting a well defined variation in latitude during ~09:17–16:20 UT on 31 August.

contracted poleward, before a broader SAPS gradually expanded equatorward. The backscatter powers were bifurcated in group range, suggesting the presence of several troughs. Again, the AWFC was established during the expansion phase. Note that other onsets preceded the study interval, so the AWFC did not necessarily commence during the growth phase.

Fig. 4 is a bar chart showing the percentage occurrence rate of AWFCs observed during each month of the year 2000. Multiple events in time and bifurcated in latitude were ignored, so the maximum occurrence rate was one event per night, or 100%. The average of the 12 monthly occurrence rates was 40%, with a standard deviation of 12%. Without corroborating evidence, the seasonal variations were not considered significant, especially considering the large variability in geomagnetic activity. A total of 98 "events" were actually observed during 260 nights of reliable radar operations. Allowing for radar down time, this implies ~146 events might have been directly observed.

The preceding occurrence rates are considered lower limits because AWFCs may have occurred, but were not observed even though the radar was operating correctly. This is because of unfavourable HF propagation conditions

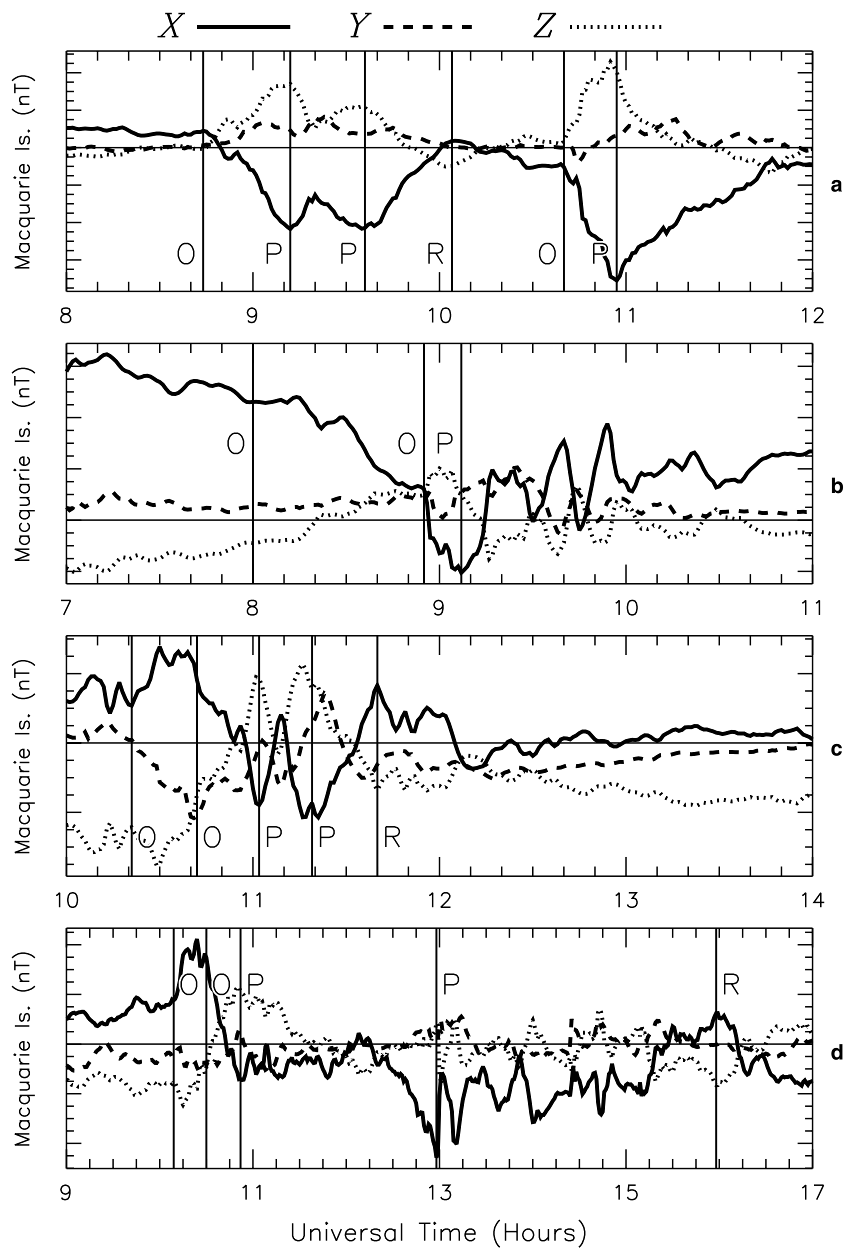

Fig. 3. Perturbations of the geomagnetic *X* (solid curve), *Y* (dashed curve), and *Z* (dotted curve) components measured by the Macquarie Island magnetometer during the same time intervals as shown in Fig. 1. Annotations indicate approximate times of substorm onset (O), peak expansion (P), and end of recovery phase (R).

or weak ionospheric irregularity production. Perhaps as many as ∼198 events may have occurred if we allow for the fraction of times no scatter was detected when the radar was operating correctly. However, this matter is problematic since AWFCs should form near strong gradients in electron density which favour enhanced HF refraction and the production of ionospheric irregularities. That is, there should be a tendency for AWFCs to be observed whenever they occur.

Other more serious corrections pertain to the AWFCs that were not observed because TIGER observed the ∼19–01 MLT sector for ∼25% of each day. Hence the duration or count of AWFCs may have been up to four times larger. Moreover, numerous AWFCs probably occurred equatorward of ∼−62° during more active intervals. This latitude is equatorward of the preferred range gate for the detection of 0.5-hop ionospheric scatter from the F-region. Referring to Figs. 2 and 5 of Karlsson et al. (1998), approximately 2/3 of events were observed equatorward of 62°. If the SuperDARN network covered all longitudes and extended further equatorward, one or more AWFCs would have been observed on nearly every night.

How does this AWFC occurrence compare with the occurrence of substorm onsets during 08–14 UT (∼19–01 MLT)? The United Kingdom Sub-Auroral Magnetometer Network (SAMNET) consists of a network of

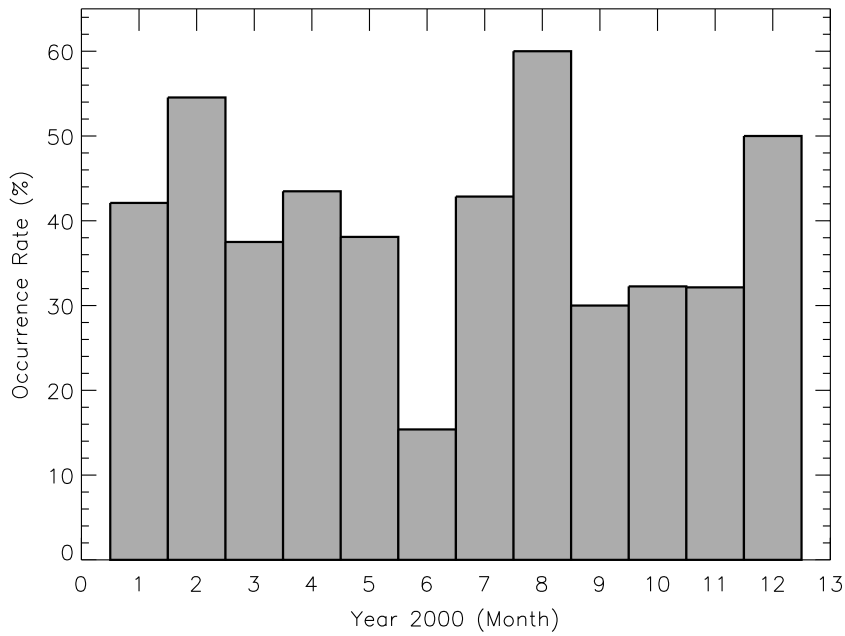

Fig. 4. Bar chart showing the percentage occurrence rate of AWFCs observed during each month of the year 2000. The occurrence rate was defined as 100% multiplied by the number of evenings an AWFC was observed divided by the number of evenings the radar was operational.

magnetometers centred near the Greenwich meridian. SAMNET data were used to identify all the substorm onset times during 2000. The longitude of SAMNET magnetometers differs by ~10 h from the longitude of TIGER. Hence the 19–01 MLT sector roughly corresponds to the interval 18–24 UT for SAMNET. A substorm onset signature was recorded on nearly every day of the year in this UT interval, similar to the occurrence of AWFCs.

The previous statistical inferences were confirmed by our survey of data recorded on individual nights. Time series of the MQI *X* component, the *AE*, and the *AL* indices were plotted for two months of data, and variations during the interval 08–14 UT were highlighted. The TIGER data were examined for the occurrence of AWFCs. Invariably, if an AWFC was not observed, the geomagnetic conditions were unusually quiet, or very disturbed (i.e., the AWFC was too far equatorward). AWFCs tended to be observed when there were isolated negative bays up to ~600 nT. However, they were not observed for more disturbed conditions, or during lesser bays following ongoing geomagnetic activity.

In summary, the results of surveying year 2000 data suggest that AWFCs were potentially observable by TIGER on up to ~150 nights, and if more radars were deployed at lower latitudes and in different longitude sectors, an AWFC would be observed at least once every night. The occurrence rates of AWFCs and substorms are similar.

3. Discussion and conclusions

A full-scan plot of the LOS velocity was only shown for the 22 April event for brevity. However, similar to the events reported by Parkinson et al. (2003, in press), our survey of year 2000 results suggests there is a tendency for the strongest AWFC echoes to be observed when looking along the flow direction. This might be caused by the generation of 10-m scale irregularities by the cascade of energy from primary gradient drift waves of much greater scale length. Likewise, the backscatter powers tended to be moderate (<25 dB), and the Doppler spectral widths either small (<60 m s) or moderate (100–250 m s) during the main flow bursts we call AWFCs, and then the powers tended to be large (20–40 dB) and the spectral widths low (<60 m s) during the subsequent SAPS. This was especially so for the "jet-like" events (e.g., Figs. 1 and 2(c)). The considerable variability in backscatter characteristics of different AWFCs needs to be reconciled with various plasma instabilities occurring in proximity to the auroral oval and main trough.

AWFCs exhibit a diverse range of morphology (e.g., Fig. 2). Sometimes the peak velocities are bifurcated, or they are concentrated in very narrow channels (<45 km) which oscillate in latitude. The complicated electric field structures driving these motions must map to the inner magnetosphere. Or at least this must be true of the longer wavelength structure (Weimer et al., 1985). In turn, there must be implications for the distribution of plasma particle populations in the inner magnetosphere which need modelling. Because these events map to the latitude of the main ionospheric trough, modelling is also required to specify the formation and evolution of the plasma trough. AWFCs may contribute to the formation of the plasmapause (Ober et al., 1997).

When deriving the plasma populations in the inner magnetosphere which result from substorm particle injections, it is common for modelers to use a highly smoothed convection pattern, such as the one given by Volland (1978). Our results show that coincident with many substorm injections, and at critical auroral and sub-auroral latitudes, a highly structured convection field exists. Even a cursory examination of DMSP measurements of transverse ion drift confirms the existence of persistent, large, westward flow structure immediately equatorward of the auroral oval in the dusk to pre-midnight sector (Parkinson et al., in press). This structure needs to be taken in to account when modeling inner magnetosphere particle populations.

It is practically impossible to show that an AWFC occurs for every substorm because radar and satellite data rarely provide continuous coverage in space and time. However, we have presented a simple but important statistical argument suggesting the occurrence rate of AWFCs is very similar to the occurrence rate of substorms. Analysis of individual events also implies an intimate link between the onset of AWFCs and substorms. We conclude the earlier case studies combined with the present statistical argument implies that AWFCs are a fundamental aspect of the substorm process.

In terms of electric field enhancements, AWFCs are the dominant ionospheric signature of substorms, and no doubt they account for a large fraction of the electric potential generated during substorms. However, there is a possibility that AWFCs and substorms may be independent phenomena, with their association a coincidence because they both occur at similar MLTs every night. That is, observations may eventually reveal a class of substorm occurring without AWFCs, and vice versa. For example, Nishitani et al. (2003) reported observation of a persistent westward flow channel during exceptionally quite geomagnetic conditions (“the day the solar wind disappeared”). The characteristics of the convection and field-aligned currents implied by the coincident DMSP particle precipitation measurements were consistent with the electrodynamics of an AWFC.

Proving cause and effect, namely whether substorms cause AWFCs or vice versa, requires further modeling combined with observations more comprehensive and reliable than presented here. The problems with HF backscatter radar measurements, namely the lack of continuity of echoes in space and time, combined with measurement errors, usually make it difficult to pinpoint the timing of events to accuracies better than a few minutes. So far we have not been able to distinguish between whether AWFCs or substorms commence first. Nor have we found unambiguous evidence for the emergence of AWFCs during the substorm growth phase.

4. Uncited reference

Parkinson et al. (2004).

Acknowledgements

This work was supported by the Australian Research Council, the Australian Antarctic Science Advisory Committee, and the Australian Academy of Sciences. Geoscience Australia is thanked for making available MQI fluxgate magnetometer data. Finally, we thank the numerous people who contributed to the operation of TIGER.

References

Anderson, P.C., Heelis, R.A., Hanson, W.B. The ionospheric signatures of rapid subauroral ion drifts. J. Geophys. Res. 96, 5,785–5,792, 1991.

Anderson, P.C., Hanson, W.B., Heelis, R.A., Craven, J.D., Baker, D.N., Frank, L.A. A proposed production model of rapid subauroral ion drifts and their relationship to substorm evolution. J. Geophys. Res. 98, 6,069–6,078, 1993.

Anderson, P.C., Carpenter, D.L., Tsuruda, K., Mukai, T., Rich, F.J. Multisatellite observations of rapid subauroral ion drifts. J. Geophys. Res. 106, 29,585–29,599, 2001.

Dyson, P.L., Devlin, J.C. The Tasman International Geospace Environment Radar. The Physicist (The Australian Institute of Physics) 37 (March/April), 48–53, 2000.

Foster, J.C., Burke, W.J. SAPS, a new categorization for sub-auroral electric fields. EOS Trans. Am. Geophys. Union 83 (36), 393–394, 2002.

Freeman, M.P., Southwood, D.J., Lester, M., Yeoman, T.K., Reeves, G.D. Substorm-associated radar auroral surges. J. Geophys. Res. 97, 12,173–12,185, 1992.

Galperin, Y.I., Ponomarev, V.N., Zosimova, A.G. Direct measurements of ion drift velocity in the upper ionosphere during a magnetic storm, 2. Results of measurements during the November 3, 1967 magnetic storm. Cosmic. Res. 11, 283–292, 1973 (in Russian).

Galperin, Y.I., Khalipov, V.L., Filippov, V.M. Signature of rapid subauroral ion drifts in the high-latitude ionosphere structure. Ann. Geophys. 4, 145–154, 1986.

Greenwald, R.A., Baker, K.B., Hutchins, R.A., Hanuise, C. An HF phased-array radar for studying small-scale structure in the high-latitude ionosphere. Radio Sci. 20, 63–79, 1985.

Greenwald, R.A., Baker, K.B., Dudeney, J.R., et al. DARN/SuperDARN: a global view of the dynamics of high-latitude convection. Space Sci. Rev. 71, 761–796, 1995.

Jayachandran, P.T., MacDougall, J.W., Donovan, E.F., Ruohoniemi, J.M., Liou, K., Moorcroft, D.R., St-Maurice, J.-P. Substorm associated changes in the high-latitude ionospheric convection. Geophys. Res. Lett. 30 (20), 2064, doi:10.1029/2003GL017497, 2003.

Karlsson, T., Marklund, G.T., Blomberg, L.G. Subauroral electric fields observed by the Freja satellite: a statistical study. J. Geophys. Res. 103, 4,327–4,341, 1998.

Nishitani, N., Papitashvili, V.O., Ogawa, T., et al. Interhemispheric asymmetry of the high-latitude ionospheric convection on 11-12 May 1999. J. Geophys. Res. 108 (A5), 1184, doi:10.1029/2002JA009680, 2003.

Ober, D.M., Horwitz, J.L., Gallagher, D.L. Formation of density troughs embedded in the outer plasmasphere by subauroral ion drift events. J. Geophys. Res. 102, 14,595–14,602, 1997.

Parkinson, M.L., Pinnock, M., Dyson, P.L., Ye, H., Devlin, J.C., Hairston, M.R. On the lifetime and extent of an auroral westward flow channel observed during a magnetospheric substorm. Ann. Geophys. 21, 893–913, 2003.

Parkinson, M.L., Chisham, G., Pinnock, M., Dyson, P.L., Devlin, J.C. Magnetic local time, substorm, and particle precipitation-related variations in the behaviour of SuperDARN Doppler spectral widths. Ann. Geophys. 22, 4103–4122, 2004.

Parkinson, M.L., Pinnock, M., Wild, J.A., Lester, M., Yeoman, T.K., Milan, S.E., Ye, H., Devlin, J.C., Frey, H.U., Kikuchi, T. Interhemispheric asymmetries in the occurrence of magnetically conjugate sub-auroral polarisation streams. Ann. Geophys. (in press).

Shand, B.A., Lester, M., Yeoman, T.K. Substorm associated radar auroral surges: a statistical study and a possible generation model. Ann. Geophys. 16, 441–449, 1998.

Spiro, R.W., Heelis, R.A., Hanson, W.B. Rapid subauroral ion drifts observed by Atmospheric Explorer C. Geophys. Res. Lett. 6, 660–663, 1979.

Volland, H.A. model of the magnetospheric electric convection field. J. Geophys. Res. 83, 2,695–2,699, 1978.

Weimer, D.R., Goertz, C.K., Gurnett, D.A., Maynard, N.C., Burch, J.L. Auroral zone electric fields from DE 1 and 2 at magnetic conjunctions. J. Geophys. Res. 90, 7,479–7,494, 1985.